

## Article

# A Framework for Economically Optimal Operation of Explosive Waste Incineration Process to Reduce NO<sub>x</sub> Emission Concentration

Sunghyun Cho <sup>1,2,†</sup>, Dongwoo Kang <sup>3,†</sup>, Joseph Sang-Il Kwon <sup>4,5</sup> , Minsu Kim <sup>1</sup>, Hyungtae Cho <sup>2</sup>, Il Moon <sup>1,\*</sup> and Junghwan Kim <sup>2,\*</sup> 

- <sup>1</sup> Department of Chemical and Biomolecular Engineering, Yonsei University, 50 Yonsei-ro, Seodaemun-gu, Seoul 03722, Korea; muckre@yonsei.ac.kr (S.C.); minsu77@yonsei.ac.kr (M.K.)
- <sup>2</sup> Green Materials & Processes R&D Group, Korea Institute of Industrial Technology, 55 Jongga-ro, Jung-gu, Ulsan 44413, Korea; htcho@kitech.re.kr
- <sup>3</sup> Department of Engineering Chemistry, Chungbuk National University, 1 Chungdae-ro, Seowon-gu, Cheongju, Chungbuk 28644, Korea; qwerty@cbnu.ac.kr
- <sup>4</sup> Artie McFerrin Department of Chemical Engineering, Texas A&M University, College Station, TX 77845, USA; kwonx075@tamu.edu
- <sup>5</sup> Texas A&M Energy Institute, Texas A&M University, College Station, TX 77845, USA
- \* Correspondence: ilmoon@yonsei.ac.kr (I.M.); kjh31@kitech.re.kr (J.K.); Tel.: +82-2-2123-2761 (I.M.); +82-52-980-6629 (J.K.)
- † These authors contributed equally to this work.



**Citation:** Cho, S.; Kang, D.; Kwon, J.S.-I.; Kim, M.; Cho, H.; Moon, I.; Kim, J. A Framework for Economically Optimal Operation of Explosive Waste Incineration Process to Reduce NO<sub>x</sub> Emission Concentration. *Mathematics* **2021**, *9*, 2174. <https://doi.org/10.3390/math9172174>

Academic Editor: Mingheng Li

Received: 20 July 2021

Accepted: 3 September 2021

Published: 6 September 2021

**Publisher's Note:** MDPI stays neutral with regard to jurisdictional claims in published maps and institutional affiliations.



**Copyright:** © 2021 by the authors. Licensee MDPI, Basel, Switzerland. This article is an open access article distributed under the terms and conditions of the Creative Commons Attribution (CC BY) license (<https://creativecommons.org/licenses/by/4.0/>).

**Abstract:** Explosives, especially those used for military weapons, have a short lifespan and their performance noticeably deteriorates over time. These old explosives need to be disposed of safely. Fluidized bed incinerators (FBIs) are safe for disposal of explosive waste (such as TNT) and produce fewer gas emissions compared to conventional methods, such as the rotary kiln. However, previous studies on this FBI process have only focused on minimizing the amount of NO<sub>x</sub> emissions without considering the operating and unitality costs (i.e., total cost) associated with the process. It is important to note that, in general, a number of different operating conditions are available to achieve a target NO<sub>x</sub> emission concentration and, thus, it requires a significant computational requirement to compare the total costs among those candidate operating conditions using a computational fluid dynamics simulation. To this end, a novel framework is proposed to quickly determine the most economically viable FBI process operating condition for a target NO<sub>x</sub> concentration. First, a surrogate model was developed to replace the high-fidelity model of an FBI process, and utilized to determine a set of possible operating conditions that may lead to a target NO<sub>x</sub> emission concentration. Second, the candidate operating conditions were fed to the Aspen Plus™ process simulation program to determine the most economically competitive option with respect to its total cost. The developed framework can provide operational guidelines for a clean and economical incineration process of explosive waste.

**Keywords:** surrogate model; NO<sub>x</sub> emissions; incineration process; fluidized bed; explosive waste; cost estimation

## 1. Introduction

Explosives are reacted under certain conditions to generate high energy; they have been used in various fields. In particular, they have been developed for military weapons with adequate quantities stockpiled for emergencies [1]. However, explosives have a short lifespan and their performance noticeably deteriorates after 10 years, despite being stored in a suitable environment [2]. These old explosives are classified as explosive waste and are subject to disposal procedures. The main concerns regarding the incineration of explosive waste are safety and the reduction of the exhaust gas produced, which can be

an environmental pollutant. Therefore, explosive waste must be carefully handled under stable conditions.

The conventional open burning/open detonation (OB/OD) method simply reacts explosive waste in an open space to dispose of it [3]. Although the OB/OD method does not require any special technology, it is highly dangerous and produces a significant amount of environmental pollutants, such as CO and NO<sub>x</sub>, owing to incomplete reactions [4–6]. In addition, this method requires a very large space and has the disadvantage of being a discontinuous process [7]. To address these problems, the use of an incinerator, which employs hot gas to dispose of explosive waste, has been proposed. The rotary kiln requires 1% of the space required by the OB/OD method and the amount of emitted exhaust gas is just 10% [8]. Although the rotary kiln is relatively efficient compared to the OB/OD method, it is still unsafe. Furthermore, hot spots persist as the main challenge with NO<sub>x</sub> emissions. A hot spot is a point where the temperature is higher than the surrounding area, which makes the reaction unstable and dangerous [9,10].

To reduce the amount of environmental pollutants in the explosive waste incineration process, the use of a fluidized bed incinerator (FBI) has been suggested and its applicability has been validated by computational fluid dynamics (CFD) program simulations [11–13]. CFD is a widely used dynamic simulation program for reactor design and calculation, which can simulate difficult and dangerous experiments [14–18]. A previous simulation of the FBI by CFD and its optimization, utilizing a surrogate model, to find the minimum NO<sub>x</sub> emissions conditions [19] was successful in reducing the NO<sub>x</sub> emissions to below the Korean standard (90 ppm). By optimizing five operating variables, an operating condition that emitted less than 34% NO<sub>x</sub> compared to that emitted by conventional methods was suggested. Although this study has become an important guideline for the use of FBI in the incineration of explosive waste, operating and capital costs were not considered.

To determine the most economically viable operating condition for a particular target NO<sub>x</sub> emission concentration, a CFD simulation of FBI process has to be numerically solved multiple times, which may take up to several hours to test one operating condition. Therefore, as an alternative method, a surrogate model was developed to determine operating conditions for a target NO<sub>x</sub> emission concentration in a computationally efficient manner [20]. Specifically, artificial neural network (ANN) was selected as the method of choice for surrogate modeling, and Latin hypercube sampling (LHS) was utilized to determine appropriate datasets because it is an efficient and unbiased sampling methodology [21–23]. The developed surrogate model decreases the time required to obtain the operating conditions for the target NO<sub>x</sub> emission concentration by at least 95% with minimal accuracy loss [19].

An economic analysis was performed based on the results of the surrogate model. During explosive waste incineration, some devices predominantly consume energy. The heater is used to heat the inlet air to the target temperature for the FBI; the major operating condition determining the energy usage of this device is temperature. The compressor pressurizes the inlet air; thus, the major operating condition determining the energy usage of this device is pressure. The inlet gas velocity affects the energy usage of both these devices and determines the flowrate of air. Therefore, the devices considered in the cost calculation are the heater and compressor. The Aspen plus software program, which is widely used for simulation and economic assessment of various processes, was used to calculate the costs of this explosive waste incineration process [24,25]. The capital and utility costs obtained from the economic assessment were used to calculate the total cost, assuming that the process was operational for 10 and 20 years. Thus, this study proposes operating conditions that economically incinerate continuously generated explosive waste.

## 2. Modeling

### 2.1. CFD Model

#### 2.1.1. Governing Equations

The governing equations of the CFD program stand on the basis of the Navier–Stokes equation. The multiphase particle in cell (MP–PIC) method was selected for the CFD approach [26–28].

$$\frac{\partial \theta_f \rho_f}{\partial t} + \nabla \cdot (\theta_f \rho_f \mathbf{u}_f) = \delta \dot{m}_p \quad (1)$$

$$\frac{\partial (\theta_f \rho_f \mathbf{u}_f)}{\partial t} + \nabla \cdot (\theta_f \rho_f \mathbf{u}_f \mathbf{u}_f) = -\nabla p + \mathbf{F} + \theta_f \rho_f \mathbf{g} + \nabla \cdot (\theta_f \boldsymbol{\tau}_f) \quad (2)$$

where  $\theta_f$  is the volume fraction of the fluid,  $\rho_f$  is the fluid density,  $\mathbf{u}_f$  is the velocity vector of the fluid,  $\delta \dot{m}_p$  is the gas mass production rate per volume from the particle–gas chemical reaction,  $p$  is the fluid pressure,  $\mathbf{F}$  is the momentum exchange rate per unit volume between the fluid and the particles,  $\mathbf{g}$  is the gravitational acceleration, and  $\boldsymbol{\tau}_f$  is the stress tensor of the fluid.

In case of the non-hydrostatic part, the constitutive equation of the stress  $\boldsymbol{\tau}_f$  is based on the deformation rate and it is obtained by the following equation:

$$S_{ij} = \frac{1}{2} \left( \frac{\partial u_i}{\partial x_j} + \frac{\partial u_j}{\partial x_i} \right) \quad (3)$$

For a Newtonian fluid, the stress can be expressed as follows:

$$\tau_{f,ij} = 2\mu S_{ij} - \frac{2}{3}\mu \delta_{ij} \frac{\partial u_k}{\partial x_k} \quad (4)$$

where,  $\mu$  is the viscosity coefficient and it is based on the fluid thermodynamic state.

The particle acceleration is calculated as follows:

$$\frac{d\mathbf{u}_p}{dt} = D_p (\mathbf{u}_f - \mathbf{u}_p) - \frac{1}{\rho_p} \nabla p + \mathbf{g} - \frac{1}{\theta_p \rho_p} \nabla \tau_p + \frac{\bar{\mathbf{u}}_p - \mathbf{u}_p}{\tau_D} \quad (5)$$

where  $D_p$  is the drag coefficient,  $\rho_p$  is the density of the particle,  $\tau_p$  is the contact stress tensor of the particle,  $\mathbf{u}_p$  is the velocity of the particle,  $\bar{\mathbf{u}}_p$  is the local mass average particle velocity,  $\tau_D$  is a particle collision damping time.

The drag function depends on fluid states, such as the drag coefficient,  $C_d$ , and the Reynolds number,  $Re$ , which is defined as

$$Re = \frac{2\rho_f r_p |\mathbf{u}_f - \mathbf{u}_p|}{\mu_f} \quad (6)$$

where  $r_p$  is the particle radius and  $\mu_f$  is the fluid viscosity.

The relation between the drag function  $D_p$  and the drag coefficient  $C_d$  is as follows:

$$D_p = \frac{3}{8} C_d \frac{\rho_f |\mathbf{u}_f - \mathbf{u}_p|}{\rho_p r_p} \quad (7)$$

In this study, the Wen–Yu/Ergun combined model was applied to calculate the drag coefficient. The Wen–Yu model uses the volume fraction of the fluid,  $\theta_f$ , to account for the drag of a single particle and particle packing. In the Wen–Yu drag model, the drag coefficient,  $C_d$ , is a function of the Reynolds number,  $Re$ ; the drag function and particle

force are calculated by Equations (5) and (7), respectively. Thus, the drag coefficient,  $C_d$ , is given as follows [29–32]:

$$C_d = \begin{cases} \frac{24}{Re} \theta_f^{n_0}, & Re < 0.5, \\ \frac{24}{Re} \theta_f^{n_0} (c_0 + c_1 Re^{n_1}), & 0.5 \leq Re \leq 1000, \\ C_2 \theta_f^{n_0}, & Re > 1000, \end{cases} \quad (8)$$

where  $c_0 = 1.0$ ,  $c_1 = 0.15$ ,  $c_2 = 0.44$ ,  $n_0 = -2.65$ , and  $n_1 = 0.687$ .

The Ergun drag model was developed to calculate dense system. The particle drag force was calculated by using Equation (5). The drag function is as follows:

$$D_p = 0.5 \left( \frac{c_1 \theta_p}{\theta_f Re} + c_0 \right) \frac{\rho_f |u_f - u_p|}{r_p \rho_p} \quad (9)$$

where  $c_0 = 2$  and  $c_1 = 180$ .

The Wen–Yu model is suitable for a diluted bed and the Ergun model is appropriate to highly packed systems. Therefore, a blended Wen–Yu/Ergun model is suggested to be applied in wide range of situation. The drag function was calculated as follows [23–26]:

$$D_p = \begin{cases} D_1, & \theta_p < 0.75\theta_{CP}, \\ (D_2 - D_1) \left( \frac{\theta_p - 0.75\theta_{CP}}{0.85\theta_{CP} - 0.75\theta_{CP}} \right), & 0.75\theta_{CP} \geq \theta_p \geq 0.85\theta_{CP}, \\ D_2, & \theta_p > 0.85\theta_{CP}. \end{cases} \quad (10)$$

### 2.1.2. Chemical Kinetic Model

We selected the widely used explosive, trinitrotoluene (TNT), for this study and employed the kinetic reaction mechanism model of TNT proposed by Min et al. (2016) [33]. Furthermore, the gas phase reaction is considered to calculate the amount of exhaust gas produced, such as NO<sub>x</sub>. For the gas phase reaction, 25 components and 131 reactions were used [34]. The kinetic reaction models detailed earlier were experimentally proved and expressed by a modified Arrhenius equation using the rate constant  $k$ , pre-exponential factor  $A$ , temperature  $T$ , integer  $n$ , and activation energy  $E_a$ :

$$k = A T^n \exp\left(-\frac{E_a}{RT}\right) \quad (11)$$

### 2.2. Surrogate Model

In this study, a surrogate model was able to decrease the computational time efficiently and assist in finding the target operating conditions quickly with high accuracy. Specifically, ANN algorithm was selected to generate the surrogate model because its accuracy and computational time is better than other methods such as polynomial or kriging. For developing an ANN surrogate model, the weight ( $w$ ) and bias ( $b$ ) factors were obtained and the following equation was used.

$$y = w_2 f(w_1 \times x + b_1) + b_2 \quad (12)$$

The tangent sigmoid function was used as the activation function [35,36]:

$$f(x) = \frac{2}{e^{-2x} + 1} - 1 \quad (13)$$

The Bayesian regularization method was used for training the ANN, as it provides a higher accuracy, while the computational requirement is similar to other methods [37,38].

### 3. Simulations

#### 3.1. CFD Simulation Specifications

In this study, a highly accurate 3D CFD model of an FBI (Figure 1) was developed using the Barracuda ver. 17. The FBI is a cylinder of radius 0.5 m and height 2 m. Area (a) discharges only gases, not solid particles such as sand and TNT; it is in contact with the atmosphere. The hot air is injected through Area (b) and the explosive waste enters through Area (c). The FBI is designed to dispose of 20,000 kg/year (0.634 g/s) of explosive waste. The initial temperature of the explosive waste particles is 300 K; the waste particles are heated by the hot air. To prevent a rapid increase in temperature of the explosive waste, it is mixed with water and injected as sludge. Furthermore, 40% of the FBI is filled with sand, which absorbs the heat and shock from the TNT incineration.

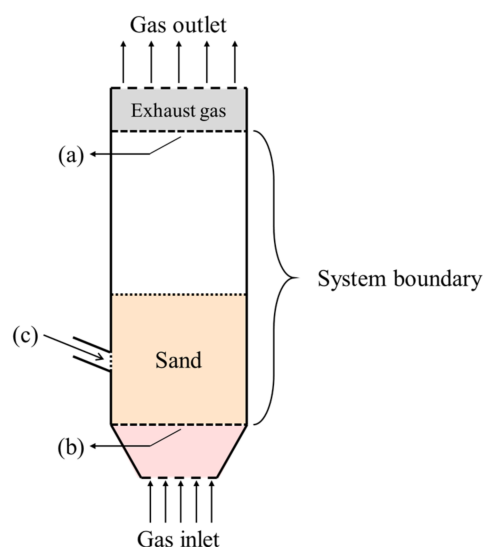


Figure 1. 3D modeling of a FBI.

For the simulation, five operating conditions that can affect the explosive waste incineration were selected: inlet gas velocity ( $v$ ), temperature ( $T$ ), pressure ( $P$ ), diameter of the explosive waste particle ( $d$ ), and mass ratio of TNT and water ( $M$ ). Table 1 lists the detailed specifications of the FBI.

Table 1. Detailed conditions of CFD simulations.

Design Conditions	
Height (m)	2.0
Diameter (m)	0.5
Sand particle size (mm)	0.26
Mass flow rate of TNT (kg/year)	20,000
Air composition (molar fraction)	N <sub>2</sub> 80%/O <sub>2</sub> 20%
Drag model	Wen–Yu/Ergun
Simulation time (s)	60
Operating conditions	
Inlet gas velocity (m/s)	1.0–3.5
Temperature (K)	400–800
Pressure (bar)	2.0–4.0
Explosive waste particle size (mm)	2.0–4.0
Mass ratio of TNT	0.25–0.75

#### 3.2. Surrogate Modeling

Surrogate modeling of CFD has usually been performed to reduce simulation time for cases wherein experiment is impossible or cost is high. This method is usually used in the

aerospace field and is useful for this study dealing with dangerous explosive waste. Surrogate modeling was performed by applying 300 datasets from the CFD simulation results. The input datasets by the sampling method (combination of the operating conditions) and output datasets by the CFD method (NOx emission concentration) are used to obtain the ANN surrogate model. A total of 300 datasets were separated for training, validation and test (i.e., 70:15:15). As a result, five input variables and one output variable are used. In the case of a hidden layer, one hidden layer and 30 hidden neurons are selected. The accuracy of the surrogate model was 99.16%, which was evaluated to be significantly high. The error rate of surrogate model was calculated by following equation.

$$\text{Error rate (\%)} = \left( 1 - \frac{\text{Result of surrogat model}}{\text{Result of CFD model}} \right) \times 100 \quad (14)$$

In addition, the detailed conditions of the surrogate model are listed in Table 2.

**Table 2.** Detailed conditions of Surrogate model.

Number of input variables	5
Number of output variables	1
Total dataset number	300
Number of training datasets	210
Number of validation datasets	45
Number of testing datasets	45
Number of hidden layers	1
Number of hidden neurons	30
Training method	Bayesian regularization
Accuracy	99.16%

Compared to a previous study, which predicted absolute NOx emissions, we calculated the concentration of NOx based on the function obtained through the surrogate model. The mass flow rate ( $\dot{m}_{\text{emission gas}}$ ) was calculated based on the volume flow rate of the exhaust gas, and the concentration of NOx was calculated using this value. The related equation is as follows.

$$\text{NOx emissions (g/s), } \dot{m}_{\text{NOx}} = f(v, T, P, d, M) \quad (15)$$

$$\text{NOx emission concentration (ppm), } C_{\text{NOx}} = \frac{f(v, T, P, d, M)}{\dot{m}_{\text{emission gas}}} \quad (16)$$

The function  $f$  is obtained by ANN surrogate model.

Furthermore, the mass flowrate of the gas emission was calculated by the inlet gas velocity ( $v$ ), temperature ( $T$ ), pressure ( $P$ ), average molar mass ( $\bar{M}_{\text{emission gas}}$ ), and the inlet gas area ( $A$ ).

$$\dot{m}_{\text{emission gas}} = \frac{v \times A \times P}{R \times T} \times \bar{M}_{\text{emission gas}} \quad (17)$$

where  $R$  is 0.082 L·atm/K·mol.

### 3.3. Cost Assessment

The explosive waste incineration process is modeled for evaluating the process cost using the Aspen plus™ software as follows (Figure 2):

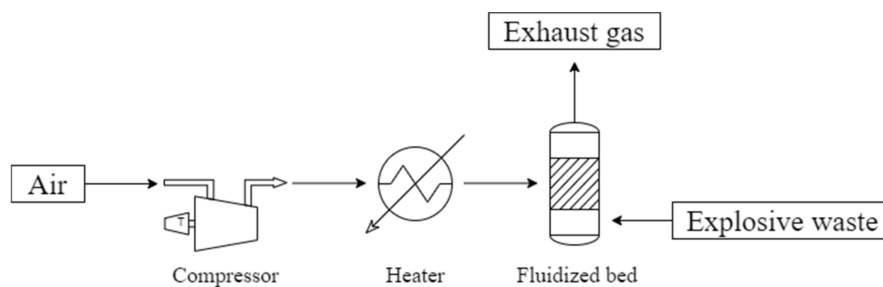


Figure 2. Simple design of the explosive waste incineration process.

First, atmospheric air (pure air) enters the compressor; it is pressurized at the target pressure, while the heater heats the air to the target temperature. Then, the hot and highly pressurized air is injected into the FBI. Finally, it makes the fluidization and helps to dispose of explosive waste in the incinerator. The volumetric flowrate was calculated based on the inlet gas velocity; it ranged from 0.031 m<sup>3</sup>/s to 0.1085 m<sup>3</sup>/s. The initial temperature and pressure were 300 K and 1.0 bar, respectively. The compressor was the isentropic type with an isentropic efficiency of 0.72 and mechanical efficiency of 1.0. It operated on electricity, which costs 0.0775 \$/kWh, whereas the heater operated on fired heat, which costs 0.0153 \$/kWh. Table 3 lists the detailed cost assessment data.

Table 3. Detailed cost assessment data.

Air Inlet		
Compressor	Volume flowrate (m <sup>3</sup> /s)	0.031–0.1085
	Temperature (K)	300
	Pressure (bar)	1.0
Heater	Compressor type	Isentropic
	Target pressure (bar)	2–4
	Utility type	Electricity
	Isentropic efficiency	0.72
	Mechanical efficiency	1.0
Heater	Target temperature (K)	400–800
	Utility type	Fired heat (400 K to 1000 K)

The integration of the above-mentioned two methods is described in Figure 3. A target NOx emission concentration was set first, and the candidate operating conditions for each target NOx were found through the developed surrogate model. The capital and utility costs were calculated by the Aspen plus software program and the minimum cost was obtained.

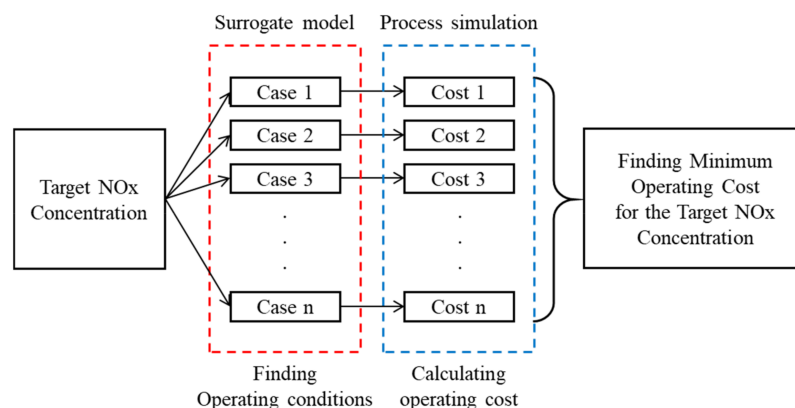


Figure 3. Combined structure of FBI surrogate model and cost assessment model for obtaining total cost for each target NOx.

#### 4. Result and Discussion

The operating condition for previous studies [19] was only focused on minimizing NOx emission concentration and, thus, the total cost was high. In this work, the target NOx emission concentration ranges from 20 ppm to 80 ppm in increments of 10. For a target NOx emission concentration, among a set of operating conditions that may lead to the target, the one that requires a minimum cost was calculated by the surrogate model (Table 4).

**Table 4.** The optimal operating conditions for various target NOx emission concentrations.

NOx Emission Concentration (ppm)	Inlet Gas Velocity (m/s)	Temperature (K)	Pressure (bar)
20	2.55	524	2.0
30	2.45	400	2.0
40	2.31	400	2.0
50	2.18	400	2.0
60	2.05	400	2.0
70	1.92	400	2.0
80	1.80	400	2.0

As stated earlier, the Aspen plus™ software program was used to simulate the cost of each operating condition, and the capital and utility costs were evaluated. The total costs for 10 and 20 years were also calculated (Table 5 and Figure 4). When the target temperature and the gas flow rate of the process were reduced, the utility cost decreased. In the case of capital cost, it was reduced when the inlet gas velocity was decreased. This is because the equipment size, capital cost, and maintenance cost are proportional to the flowrate of inlet gas.

**Table 5.** Cost information for each NOx emission concentration target.

NOx Emission Concentration (ppm)	Capital Cost (\$)	Utility Cost (\$/Year)	Total Cost (10 Years, \$)	Total Cost (20 Years, \$)
20	3,122,600	46,885	3,591,445	4,060,291
30	2,993,070	43,524	3,428,310	3,863,550
40	2,942,755	40,607	3,348,824	3,754,892
50	2,909,551	40,032	3,309,872	3,710,192
60	2,879,532	39,617	3,275,700	3,671,867
70	2,849,405	39,203	3,241,430	3,633,456
80	2,819,391	38,789	3,207,276	3,595,161

The inlet gas velocity decreased when the target NOx emission concentration was increased. This phenomenon occurs because the degree of fluidization (between explosive waste and gas) is determined by inlet gas velocity and, thus, NOx emission concentration may increase if the FBI is not well mixed at a low inlet gas velocity.

In summary, a methodology is developed for an FBI process to quickly determine the most economically optimal operating condition for a target NOx emission concentration through an ANN surrogate model and the Aspen Plus™ process simulation program. The developed framework suggests an operating condition for the FBI process to dispose of explosive waste at a cost less than the current practice. Furthermore, the study is significant as it provides operational guidelines for the design of a clean and economical incineration process to handle explosive waste subject to environmental regulation.

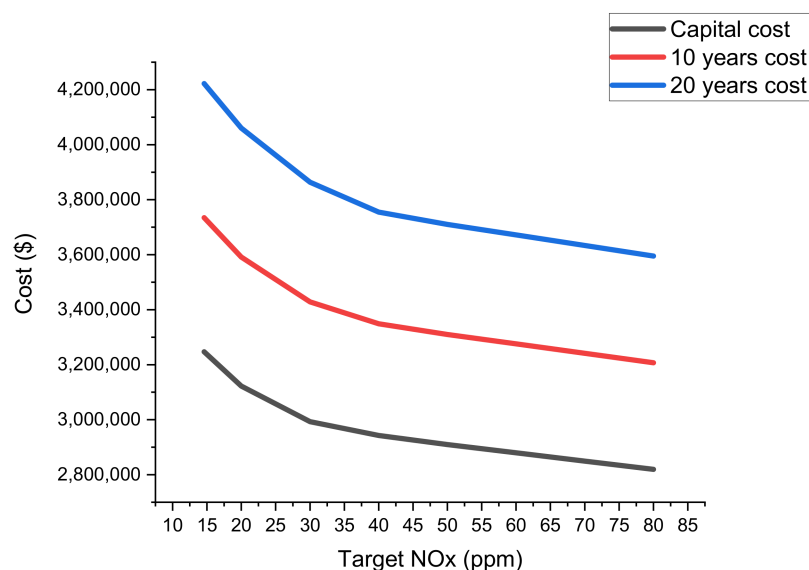


**Figure 4.** Cost change with target NOx emission concentration.

## 5. Conclusions

This study aimed at providing a methodology to determine the optimal operating conditions for safe handling of the explosive waste via an FBI process at minimal capital and utility costs. The ANN surrogate model, which utilizes process data generated by the CFD model, was used to determine the operating conditions required to yield the target NOx emission concentrations in a computationally efficient manner. Once the operating conditions were obtained via the surrogate model, the capital and utility costs were calculated using the Aspen Plus™ process simulation program. As a result of obtaining the minimum total cost for each target NOx emission concentration, the total cost decreased when the NOx emission concentration was alleviated. This study is timely and significant as it suggests a systematic framework to determine the most economically viable operating condition for handling explosive waste, while meeting the environmental regulation provided by the government. Additionally, the developed framework can be used as a platform to test the feasibility of alleviating or tightening by simultaneously considering economic and environmental considerations.

**Author Contributions:** Conceptualization, S.C.; methodology, S.C.; software, M.K.; validation, D.K., J.S.-I.K. and J.K.; formal analysis, D.K.; investigation, H.C.; resources, H.C.; data curation, S.C.; writing—original draft preparation, S.C.; writing—review and editing, D.K., J.S.-I.K., I.M. and J.K.; visualization, S.C. and D.K.; supervision, I.M. and J.K.; project administration, H.C. and J.K.; funding acquisition, H.C. and J.K. All authors have read and agreed to the published version of the manuscript.

**Funding:** This work was supported by the Korean Institute of Industrial Technology within the framework of the following projects: “Development of Global Optimization System for Energy Process [grant number EM-21-0022, IR-21-0029, IZ-21-0052]” and “Development of AI Platform Technology for Smart Chemical Process [grant number JH-21-0005]”.

**Institutional Review Board Statement:** Not applicable.

**Informed Consent Statement:** Not applicable.

**Data Availability Statement:** Not applicable.

**Conflicts of Interest:** The authors declare no conflict of interest.

## References

1. Sikder, A.K.; Sikder, N. A review of advanced high performance, insensitive and thermally stable energetic materials emerging for military and space applications. *J. Hazard. Mater.* **2004**, *112*, 1–15. [[CrossRef](#)] [[PubMed](#)]
2. Vogelsanger, B. Chemical stability, compatibility and shelf life of explosives. *Chimia* **2004**, *58*, 401–408. [[CrossRef](#)]
3. Maleki, N. Treatment and Biodegradation of High Explosives. Master's Thesis, University of California, Los Angeles, CA, USA, 1994.
4. Siddhamshetty, P.; Ahammad, M.; Hasan, R.; Kwon, J. Understanding wellhead ignition as a blowout response. *Fuel* **2019**, *243*, 622–629. [[CrossRef](#)]
5. Yuan, Z.; Meng, L.; Gu, X.; Bai, Y.; Cui, H.; Jiang, C. Prediction of NO<sub>x</sub> emissions for coal-fired power plants with stacked-generalization ensemble method. *Fuel* **2021**, *289*, 119748. [[CrossRef](#)]
6. Yang, R.; Ma, C.; Chen, G.; Cheng, Z.; Yan, B.; Mansour, M. Study on NO<sub>x</sub> emission during corn straw/sewage sludge co-combustion: Experiments and modelling. *Fuel* **2021**, *285*, 119208. [[CrossRef](#)]
7. Burrows, D.L.P.E.P.; Rosenblatt, D.H.; Mitchell, W.R. Organic Explosives and Related Compounds. *Environ. Health Consid.* **1989**. [[CrossRef](#)]
8. Duijm, N.J. Hazard analysis of technologies for disposing explosive waste. *J. Hazard. Mater.* **2002**, *90*, 123–135. [[CrossRef](#)]
9. Lee, S.-H.; Baek, S.-W.; Moon, I.; Park, J.-S.; Oh, M. Incineration Process of Double Base Propellant for Demilitarization. *Clean Technol.* **2016**, *22*, 190–195. [[CrossRef](#)]
10. Cho, S.; Park, C.; Lee, J.; Lyu, B.; Moon, I. Finding the best operating condition in a novel process for explosive waste incineration using fluidized bed reactors. *Comput. Chem. Eng.* **2020**, *142*, 107054. [[CrossRef](#)]
11. Gødde, M.; Conrad, R. Immediate and adaptational temperature effects on nitric oxide production and nitrous oxide release from nitrification and denitrification in two soils. *Biol. Fertil. Soils* **1999**, *30*, 33–40. [[CrossRef](#)]
12. Jeon, S.W.; Yoon, W.J.; Baek, C.; Kim, Y. Minimization of hot spot in a microchannel reactor for steam reforming of methane with the stripe combustion catalyst layer. *Int. J. Hydrog. Energy* **2013**, *38*, 13982–13990. [[CrossRef](#)]
13. Anastasov, A.I. A study of the influence of the operating parameters on the temperature of the hot spot in a fixed bed reactor. *Chem. Eng. J.* **2002**, *86*, 287–297. [[CrossRef](#)]
14. Cho, H.; Cha, B.; Kim, S.; Ryu, J.; Kim, J.; Moon, I. Numerical analysis for particle deposit formation in reactor cyclone of residue fluidized catalytic cracking. *Ind. Eng. Chem. Res.* **2013**, *52*, 7252–7258. [[CrossRef](#)]
15. Kim, J.; Lim, W.; Lee, Y.; Kim, S.; Park, S.R.; Suh, S.K.; Moon, I. Development of corrosion control document database system in crude distillation unit. *Ind. Eng. Chem. Res.* **2011**, *50*, 8272–8277. [[CrossRef](#)]
16. Kim, J.; Tak, K.; Moon, I. Optimization of procurement and production planning model in refinery processes considering corrosion effect. *Ind. Eng. Chem. Res.* **2012**, *51*, 10191–10200. [[CrossRef](#)]
17. Kwon, J.S.I.; Sitapure, N.; Epps, R.W.; Abolhasani, M. Cfd-based computational studies of quantum dot size control in slug flow crystallizers: Handling slug-to-slug variation. *Ind. Eng. Chem. Res.* **2021**, *60*, 4930–4941. [[CrossRef](#)]
18. Crose, M.; Kwon, J.S.; Nayhouse, M.; Ni, D.; Christofides, P.D. Multiscale modeling and operation of PECVD of thin film solar cells. *Chem. Eng. Sci.* **2015**, *136*, 50–61. [[CrossRef](#)]
19. Cho, S.; Kim, M.; Lyu, B.; Moon, I. Optimization of an explosive waste incinerator via an artificial neural network surrogate model. *Chem. Eng. J.* **2021**, *407*, 126659. [[CrossRef](#)]
20. Kwon, H.; Oh, K.C.; Choi, Y.; Chung, Y.G.; Kim, J. Development and application of machine learning-based prediction model for distillation column. *Int. J. Intell. Syst.* **2021**, *36*, 1970–1997. [[CrossRef](#)]
21. del Pecchia, M.; Fontanesi, S. A methodology to formulate multicomponent fuel surrogates to model flame propagation and ignition delay. *Fuel* **2020**, *279*, 118337. [[CrossRef](#)]
22. Poon, H.M.; Pang, K.M.; Ng, H.K.; Gan, S.; Schramm, J. Development of multi-component diesel surrogate fuel models-Part II: Validation of the integrated mechanisms in 0-D kinetic and 2-D CFD spray combustion simulations. *Fuel* **2016**, *181*, 120–130. [[CrossRef](#)]
23. Lee, D.; Singla, A.; Wu, H.J.; Kwon, J.S.I. An integrated numerical and experimental framework for modeling of CTB and GD1b ganglioside binding kinetics. *AIChE J.* **2018**, *64*, 3882–3893. [[CrossRef](#)]
24. Choi, Y.; Kim, J.; Moon, I. Simulation and economic assessment of using H<sub>2</sub>O<sub>2</sub> solution in wet scrubber for large marine vessels. *Energy* **2020**, *194*, 116907. [[CrossRef](#)]
25. Lee, J.; Cho, H.; Moon, I.; Lubomirsky, I.; Kaplan, V.; Kim, J.; Ahn, Y. Techno-economic assessment of carbonate melt flue gas desulfurization process. *Comput. Chem. Eng.* **2021**, *146*, 107227. [[CrossRef](#)]
26. Snider, D.; Guenther, C.; Dalton, J.; Williams, K. CPFD Eulerian-Lagrangian Numerical Scheme Applied to the NETL Bench-top Chemical Looping Experiment. Conference on Chemical Looping. 2010. Available online: <http://scholar.google.com/scholar?hl=en&btnG=Search&q=intitle:CPFD+Eulerian-Lagrangian+Numerical+Scheme+Applied+to+the+NETL+Bench-top+Chemical+Looping+Experiment#0> (accessed on 19 July 2021).
27. Feng, M.; Li, F.; Wang, W.; Li, J. Parametric study for MP-PIC simulation of bubbling fluidized beds with Geldart A particles. *Powder Technol.* **2018**, *328*, 215–226. [[CrossRef](#)]
28. Siddhamshetty, P.; Mao, S.; Wu, K.; Kwon, J.S.-I. Multi-Size Proppant Pumping Schedule of Hydraulic Fracturing: Application to a MP-PIC Model of Unconventional Reservoir for Enhanced Gas Production. *Processes* **2020**, *8*, 570. [[CrossRef](#)]
29. Wen, C.Y. Mechanics of fluidization. *Chem. Eng. Prog. Symp. Ser.* **1966**, *62*, 100–111.

30. Ergun, S. Fluid flow through packed columns. *Chem. Eng. Prog.* **1952**, *48*, 89–94.
31. Gidaspow, D. Multiphase Flow and Fluidization. *Contin. Kinet. Theory Descr.* **1994**, 706. Available online: <http://oreilly.com/catalog/errata.csp?isbn=9781449340377> (accessed on 19 July 2021).
32. Patel, M.K.; Pericleous, K.; Cross, M. Numerical Modelling of Circulating Fluidized Beds. *Int. J. Comput. Fluid Dyn.* **1993**, *1*, 161–176. [[CrossRef](#)]
33. Kim, S.H.; Nyande, B.W.; Kim, H.S.; Park, J.S.; Lee, W.J.; Oh, M. Numerical analysis of thermal decomposition for RDX, TNT, and Composition B. *J. Hazard. Mater.* **2016**, *308*, 120–130. [[CrossRef](#)] [[PubMed](#)]
34. Ermolin, N.E.; Zarko, V.E. Investigation of the properties of a kinetic mechanism describing the chemical structure of RDX flames. I. Role of individual reactions and species, Combustion. *Explos. Shock Waves* **2001**, *37*, 123–147. [[CrossRef](#)]
35. Hajduk, Z. Hardware implementation of hyperbolic tangent and sigmoid activation functions. *Bull. Pol. Acad. Sci. Tech. Sci.* **2018**, *66*, 563–577. [[CrossRef](#)]
36. Zadeh, M.R.; Amin, S.; Khalili, D.; Singh, V.P. Daily Outflow Prediction by Multi Layer Perceptron with Logistic Sigmoid and Tangent Sigmoid Activation Functions. *Water Resour. Manag.* **2010**, *24*, 2673–2688. [[CrossRef](#)]
37. Foresee, F.D.; Hagan, M.T. Gauss-Newton approximation to bayesian learning. *IEEE Int. Conf. Neural Netw.-Conf. Proc.* **1997**, *3*, 1930–1935. [[CrossRef](#)]
38. MacKay, D.J.C. Bayesian Interpolation. *Neural Comput.* **1992**, *4*, 415–447. [[CrossRef](#)]